Ion Pair S_N2 Reactions at Nitrogen: A High-Level G2M(+) Computational Study

Yi Ren*,† and San-Yan Chu*,‡

College of Chemistry, Sichuan University, Chengdu 610064, PRC, and Department of Chemistry, National Tsing Hua University, Hsinchu 30013, Taiwan

Received: April 15, 2004; In Final Form: June 10, 2004

The gas-phase ion pair S_N2 reactions at nitrogen, $LiY + NH_2X \rightarrow NH_2Y + LiX$ (Y, X = F, Cl, Br, or I), with inversion mechanisms are investigated at the level of modification of G2 theory, and the results are compared with two related reactions ($Y^- + NH_2X$ and $LiY + CH_3X$). Calculated results show that the $LiY + NH_2X$ reactions are exothermic only when the nucleophile is a heavier lithium halide. The complexation enthalpies are found to depend primarily on the identity of nucleophile LiY and only to a small extent on the identity of NH_2X, decreasing in the order LiI > LiBr > LiCl > LiF. Including a Li cation in the anionic S_N2 model will raise the overall barriers for the $LiY + NH_2X$ (Y, X = F−Br) reactions and lower the overall barriers for the $LiI + NH_2X$ (X = F−I) reactions. Another interesting feature of the ion pair reactions at nitrogen is the good correlation between the reaction barriers with the geometrical looseness of Li−Y and N−X bonds in the transition-state structures. The data for the reaction barriers show good agreement with the prediction of the Marcus equation and its modification. Kinetic, thermodynamic investigations and NBO analyses predict that the nucleophilicities of LiY in the gas-phase ion pair S_N2 reactions at nitrogen decrease in the order LiI > LiBr > LiCl > LiF.

1. Introduction

Displacement reactions at heteroatoms are featured widely in both organic and bioorganic chemistry, and they are among the most important processes in metabolism.[1] Recently, theoretical and experimental investigations have been devoted to anionic S_N2 reactions on heteroatoms in the gas phase, including nitrogen,[2a−e] sulfur,[3a−c] oxygen,[4] and phosphorus,[5] or in aqueous acetonitrile.[6] However, most of the S_N2 reactions in the solution phase may actually involve neutral ion pairs as reactants, which are the source of the nucleophilic anion species. The nucleophile of neutral ion pairs is expected to have a reactivity that is rather different than that of the anion species. Up to now, the ion pair S_N2 reactions have received less attention, even though there are some experimental results.[7a,b] A few theoretical studies have been done on the ion pair S_N2 reactions. Harder and co-workers[8] computed some identity ion pair S_N2 reactions at carbon at the MP4/6-31+G*//HF/6-31+G* level and found some interesting results. The calculated identity reactions of methyl fluoride and chloride with lithium and sodium fluoride and chloride involve the preliminary encounter of dipole−dipole complexes instead of a negatively charged ion−dipole complex in anionic S_N2 reactions. The reaction, then, proceeds via a cyclic inversion or retention transition structure with highly bent X−C−X bonds, behaving as assemblies of ions. Streitwieser et al.[9] extended the work to the higher alkyls by the RHF, MP2, and B3LYP methods with the 6-31+G* basis set and discussed some steric effects of the ion pair displacement reactions. Leung et al.[10] reported a theoretical study on the ion pair S_N2 reactions of metal cyanates and methyl halides. More recently, Ren and Chu completed a comprehensive investigation[11a] of the identity ion pair S_N2 reactions $LiX + CH_3X$ (X = F, Cl, Br, or I) in the gas phase and in solution at the G2M(+) level.

In our previous paper,[11b] the mechanistic studies of some identity ion pair S_N2 reactions at nitrogen (eq 1) were performed.

$$LiX + NH_2X \rightarrow NH_2X + LiX \text{ (X = F, Cl, Br, or I)} \quad (1)$$

Two possible reaction pathways via different complexes and transition states were proposed. In the inversion pathway, the incoming LiY attacks the central nitrogen atom from the backside of the leaving group, reaching the "N-philic" complex **1** (C_s). The reaction progresses as the LiX moiety moves toward the nitrogen atom, forming TS **2** (C_{2v}). For the alternative retention pathway, the lithium cation complexes with the halogen at NH_2X to form the "X-philic" prereaction complex **1′** (C_1). Then, the system proceeds to the C_s retention transition state **2′**, where the coordination of the lithium cation is on the same side of the nitrogen to both entering and leaving halide ions. Calculated results indicate that the inversion mechanism is energetically favorable compared to the retention mechanism for all of the halogens. The barrier gaps between the two mechanisms increase in the order 33.4 (X = F) < 110.5 (X = Cl) < 121.5 (X = Br) < 131.4 kJ/mol (X = I). The introduction of the Li^+ will raise the barriers for the $LiX + NH_2X$ (X = F−Br) reactions and lower the barrier for the $LiI + NH_2I$ reaction relative to the corresponding anionic reaction.

The aim in this study is to extend our investigation into the nonidentity reactions (eq 2) using a higher-level G2M(+) theory and, moreover, to test the reliability of the Marcus theory in the ion pair S_N2 reactions at nitrogen. The nucleophilicities of lithium halides are also discussed by the kinetic, thermodynamic investigations and the NBO analyses. Only the favorable inversion pathway is considered here.

$$LiY + NH_2X \rightarrow NH_2Y + LiX \quad (Y \neq X;\ Y, X = F, Cl, Br, \text{ or I}) \quad (2)$$

* To whom correspondence should be addressed.
† Sichuan University.
‡ National Tsing Hua University.

10.1021/jp048345h CCC: $27.50
Published on Web 07/24/2004

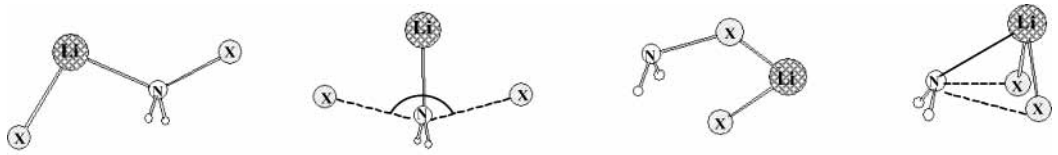

2. Methodology

The modified GAUSSIAN2 theory that was introduced by Mebel and co-workers,[13] which has been extensively used in the study of reaction mechanisms,[14a−c] was applied to this work. Previous studies[15] indicated that the diffusion function was necessary in the structure optimization for the S_N2 reaction. Therefore, the geometries of the reactants, complexes, and transition states in the title reactions had been fully optimized using the hybrid density functional B3LYP method[16a−c,17] with the 6-311+G(d,p) basis set instead of the 6-311G(d,p) basis set in the original G2M. Vibrational frequencies were employed to characterize the stationary points, and the calculated zero-point energies (ZPEs) were included in the comparison of relative energies. Electron correlation effects were evaluated using coupled-cluster calculations, including triple excitations noniteratively [CCSD(T)]. This level of theory is termed G2M-(+), in which the "(+)" stands for the addition of a diffuse function to the basis set used in obtaining the reference geometries. Details of the procedure can be found in ref 13.

All of the calculations were performed with the GAUSSIAN98 package.[18] All electron (AE) calculations were run for the first- and second-row elements, while Hay and Wadt effective core potentials[19] were used for the bromine- and iodine-containing species, termed G2M(+)-ECP. Charges were calculated by the natural bond orbital (NBO) analysis[20a−d] at the MP2/6-311+G(3df,2p) level on B3LYP/6-311+G(d,p) geometries.

Calculated total energies for all of the species are presented in Table 1. All of the G2M(+) relative energies are listed in Tables 2 and 3. The selected second-order perturbative estimates of donor−acceptor interactions, $E(2)$, are summarized in Table 5. The main geometries of all of the species are shown in Figure 1. All of the Cartesian coordinates of the optimized structures involved in the LiY + NH_2X (Y, X = F−I) reactions are given in the Supporting Information.

TABLE 1: Calculated G2M(+) Total Energies (au) for Species Involved in the Ion Pair S_N2 Reactions of LiY + NH_2X (Y, X = F−I)

species	energy	species	energy
LiF	−107.29530	reactant complex **1**	
LiCl	−467.29382	FLi···NH_2F	−262.87033
LiBr	−20.70026	ClLi···NH_2Cl	−982.89490
LiI	−18.90627	BrLi···NH_2Br	−89.71705
NH_2F	−155.54946	ILi···NH_2I	−86.14331
NH_2Cl	−515.57321	ClLi···NH_2F	−622.87105
NH_2Br	−68.98769	BrLi···NH_2F	−176.27828
NH_2I	−67.207033	ILi···NH_2F	−174.48485
inversion TS **2**		BrLi···NH_2Cl	−536.30236
[LiF/NH_2F]‡	−262.81078	ILi···NH_2Cl	−534.50903
[LiCl/NH_2Cl]‡	−982.85248	ILi···NH_2Br	−87.92387
[LiBr/NH_2Br]‡	−89.68592	product complex **3**	
[LiI/NH_2I]‡	−86.11985	FLi···NH_2Cl	−622.89329
[LiCl/NH_2F]‡	−622.83028	FLi···NH_2Br	−176.30757
[LiBr/NH_2F]‡	−176.24553	FLi···NH_2I	−174.52647
[LiI/NH_2F]‡	−174.45968	ClLi···NH_2Br	−536.30945
[LiBr/NH_2Cl]‡	−536.26880	ClLi···NH_2I	−534.52896
[LiI/NH_2Cl]‡	−534.48399	BrLi···NH_2I	−87.93654
[LiI/NH_2Br]‡	−87.90170		

Throughout this paper, bond lengths are in angstroms and bond angles are in degrees. Relative energies correspond to enthalpy changes at 0 K [ΔH(0 K)] in kilojoules per mole.

3. Results and Discussion

The gas-phase reaction energy profile for the concerted ion pair S_N2 reactions at nitrogen (eq 2) is described by an asymmetrical double-well curve for the nonidentity reactions (Scheme 1). The reaction involves the initial formation of a reactant dipole−dipole complex **1**. The complex must then overcome the central barrier to reach an asymmetrical transition structure **2**, in which the Li−Y and N−X bonds become longer. In addition, the attacking halogen atom Y is closer to nitrogen, X moves away from nitrogen, and the lithium atom moves toward X, reaching the product dipole−dipole complex **3**, which subsequently dissociates into the separate products.

Analyses of the overall enthalpy changes indicate that the gas-phase nonidentity ion pair S_N2 reactions at nitrogen are exothermic only if the nucleophile is a heavier lithium halide, which is different from the situation in the nonidentity anionic S_N2 reactions $Y^- + CH_3X \rightarrow CH_3Y + X^-$ [21] and $Y^- + NH_2X \rightarrow NH_2Y + X^-$ (Y, X = F−I),[2c] where the reactions are exothermic only if the nucleophile is the lighter halide. The forward reactions are defined as exothermic in the following discussion.

The key energetic quantities involved in the reactions (eq 2), depicted in Scheme 1, are labeled as follows: ΔH^{comp}_{YX} and ΔH^{comp}_{XY} are the complexation enthalpies for the dipole−dipole complexes **1** and **3**, respectively. $\Delta H^{‡}_{YX}$ and $\Delta H^{‡}_{XY}$ are the central activation barriers, and ΔH^{b}_{YX} and ΔH^{b}_{XY} are the overall activation barriers for the corresponding forward and reverse reactions. ΔH is the central enthalpy difference between the product and reactant ion−molecule complexes **1** and **3**. ΔH^{ovr} is the overall enthalpy change for the forward reaction.

A. LiX and NH_2X Structures (X = F, Cl, Br, or I). Calculated geometries and predicted properties of LiX and NH_2X were presented in our previous paper.[11b] B3LYP/6-311+G(d,p) geometries generally agree well with the available experimental data and MP2/6-31+G(d) results. All of the frequencies, dipole moment values, and Li−X bond dissociation energies for LiX are reproduced by the DFT method.

B. Dipole−Dipole Complexes. When the the reactant dipole−dipole complex **1** is formed, lithium coordinates with nitrogen to form complexes YLi···NH_2X, and there are simultaneously weak electrostatic interactions between the attacking halogen atom Y and two hydrogen atoms, which is much different from the complexes Y^-···HNHX in the anionic S_N2

TABLE 2: G2M(+) Complexation Enthalpies (kJ/mol) of the Dipole−Dipole Complexes, 1 and 3

	LiF	LiCl	LiBr	LiI
NH_2F	67.1 (114.0)[a]	72.9	75.0	76.5
NH_2Cl	65.1	73.2 (67.8)	75.9	77.6
NH_2Br	64.5	73.4	76.4 (58.4)	78.5
NH_2I	63.4	73.8	76.8	78.8 (50.0)

[a] Values in parentheses are the G2M(+) complexation energies for $X^- + NH_2X \rightarrow NH_2X + X^-$ reactions (X = F−I) from ref 2a.

TABLE 3: Central Barrier Heights ($\Delta H^{\ddagger}_{YX}$ and $\Delta H^{\ddagger}_{XY}$), Overall Barrier Heights (ΔH^{b}_{YX} and ΔH^{b}_{XY}), Enthalpy Differences between Reactant and Product Dipole−Dipole Complexes (ΔH), and Overall Reaction Enthalpies (ΔH^{ovr}) for Exothermic LiY + NH_2X (Y, X = F−I) Reactions at the G2M(+) Level (kJ/mol)

Y, X	$\Delta H^{\ddagger}_{YX}$	ΔH^{b}_{YX}	ΔH^{b}_{XY}	$\Delta H^{\ddagger}_{XY}$	ΔH	ΔH^{ovr}
F, F	156.3 (58.2)[a]	89.2 (−55.8)				
	263.6[b]	*204.7*				
Cl, Cl	111.4 (58.5)	38.2 (−9.3)				
	203.3	*146.9*				
Br, Br	81.7 (44.7)	5.3 (−13.7)				
	174.7	*119.0*				
I, I	61.6 (39.1)	−17.2 (−10.8)				
	150.7	*97.3*				
Cl, F	107.0, **106.3**[c]	34.1, **32.6**	100.4, **98.9**	165.4, **164.6**	−58.4	−66.3
		180.6[d] **(−4.0)**[e]	***171.1*** **(−55.5)**			
Br, F	86.0, **83.7**	11.0, **7.6**	98.4, **95.0**	162.9, **160.6**	−76.9	−87.4
		166.2 **(1.7)**	***157.6*** **(−61.5)**			
I, F	66.1, **61.2**	−10.4, **−16.6**	112.0, **105.8**	175.3, **170.5**	−109.3	−122.4
		149.8 **(−1.0)**	***152.2*** **(−57.4)**			
Br ,Cl	88.1, **87.5**	12.2, **11.5**	33.4, **32.6**	106.7, **106.1**	−18.6	−21.1
		132.5 **(−5.5)**	***133.4*** **(−17.2)**			
I, Cl	65.7, **62.3**	−11.9, **−15.3**	44.3, **40.8**	118.1, **114.6**	−52.3	−56.1
		116.2 **(−7.5)**	***128.1*** **(−12.5)**			
I, Br	58.2, **56.0**	−20.3, **−22.4**	14.7, **12.6**	91.5, **89.3**	−33.3	−35.0
		102.7 **(−15.6)**	***113.7*** **(−8.8)**			

[a] Values in parentheses are G2M(+) energies of the $X^- + NH_2X$ (X = F−I) reactions from ref 2a. [b] Values in italics are G2M(+) energies of the $LiX + CH_3X$ (X = F−I) reactions from ref 11a. [c] Values in bold are the estimated central barriers by eq 6 and overall barriers by eq 7 for the nonidentity reactions $LiY + NH_2X$ (Y ≠ X; Y, X = F−I). [d] The bold values in italic are the estimated overall barriers by eq 7 for the nonidentity reactions $LiY + CH_3X$ (Y ≠ X; Y, X = F−I). [e] The bold values in parentheses are the estimated overall barriers by eq 7 for the nonidentity reactions $Y^- + NH_2X$ (Y ≠ X; Y, X = F−I) using the data in ref 2a.

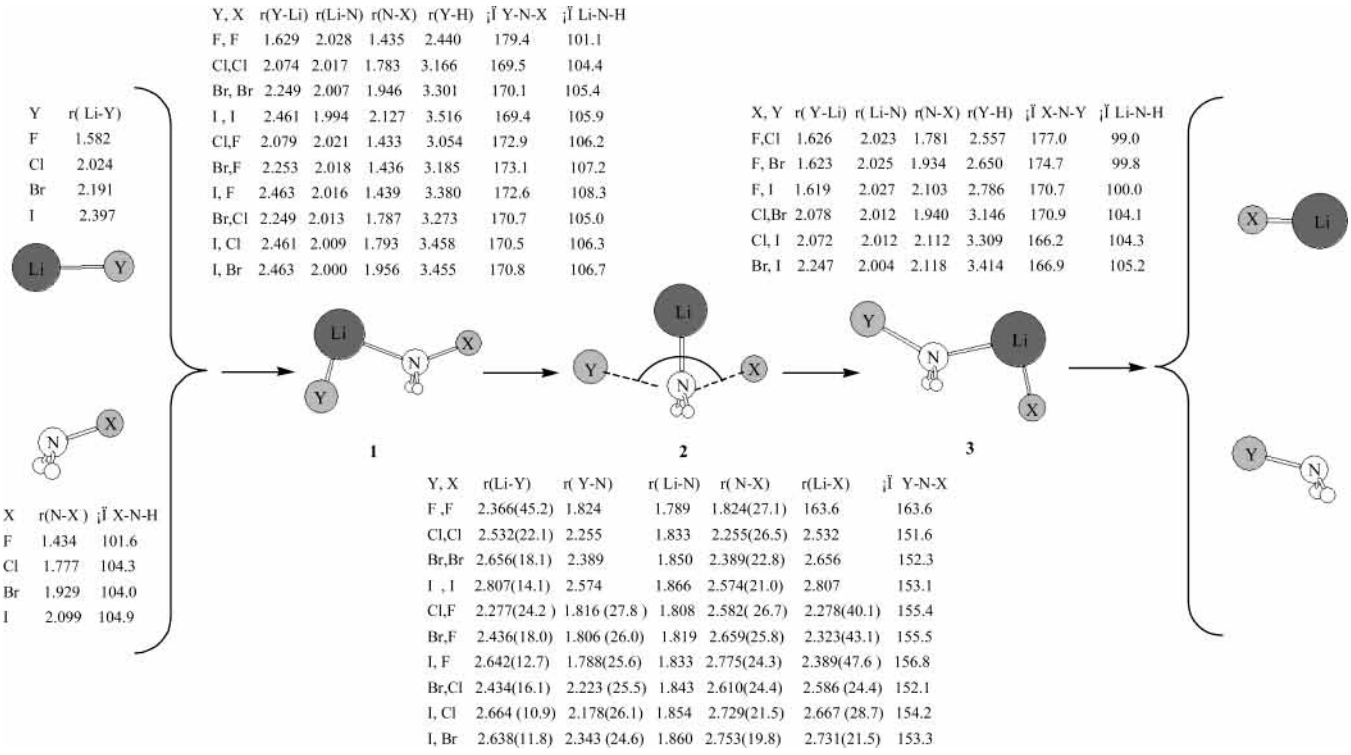

Figure 1. Main geometries of the reactants, dipole−dipole complexes, and transition-state structures in the gas-phase reactions LiY + NH_2X (Y, X = F−I) at the B3LYP/6-311+G(d,p) level. The data in parentheses are the geometrical looseness for the corresponding bonds.

reactions at nitrogen,[2a,c] where the halide ion coordinates with just one hydrogen.

The G2M(+) complexation enthalpies, ΔH^{comp}_{YX}, for complexes $YLi\cdots H_2X$ (Y, X = F−I) in Table 2 indicate that the complexation enthalpies depend primarily on the identity of LiY and only to a smaller extent on the identity of NH_2X. They tend to decrease in the order LiI > LiBr > LiCl > LiF, in contrast to those for the corresponding gas-phase anionic S_N2 reactions at nitrogen, $Y^- + NH_2X$,[2c] where the complexation enthalpies decrease in the basicity order $F^- > Cl^- > Br^- > I^-$. Thus, the complexation enthalpies with different NH_2X species range between 63.4 and 67.1 kJ/mol for LiF, 72.9 and 73.8 kJ/mol for LiCl, 75.0 and 76.8 kJ/mol for LiBr, and 76.5 and 78.8 kJ/mol for LiI. Previous studies pointed out that the stabilization energies for complexes $XLi\cdots NH_2X$ may be mainly attributed to the interaction of the lithium cation and nitrogen atom. It can be seen from Figure 1 that when NH_2X is fixed, the Li−N distances in complexes $YLi\cdots NH_2X$ (Y = F−I) decrease with the order LiF > LiCl > LiBr > LiI. For example, the Li−N distance decreases from 2.028 Å for LiF to 2.016 Å

SCHEME 1: Schematic Potential Energy Surface for the LiY + NH_2X Nonidentity Ion Pair S_N2 Reactions at Nitrogen (eq 2)

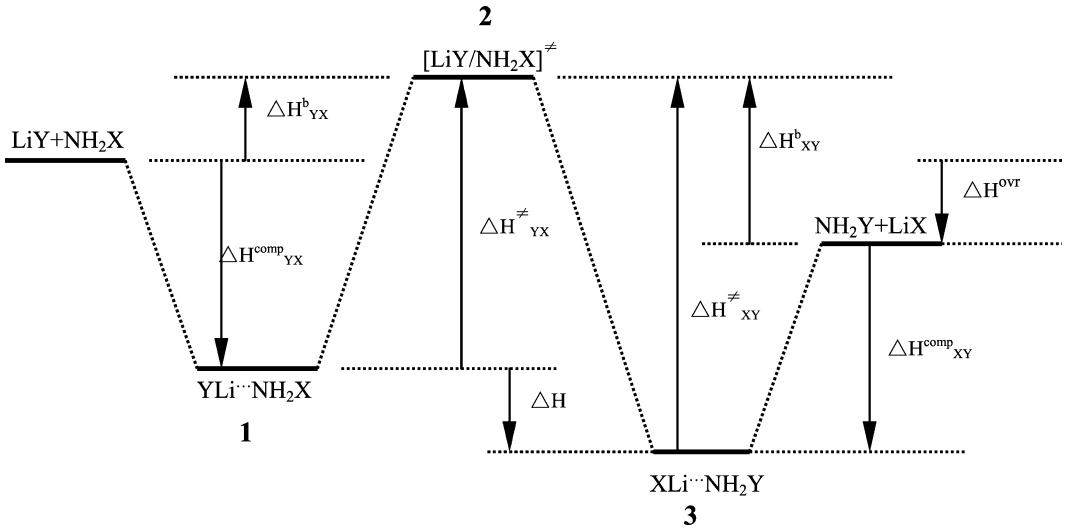

for LiI in the complexes YLi···NH_2F (Y = F−I). The shorter Li−N distance will lead to the stronger interaction between the lithium and nitrogen atoms. For a given LiY, the complexation enthalpy correlates well with the electronegativity of X (e.g., $R^2 = 0.984$ for NH_2I, and coefficients are even greater for the other amino halides). If LiY is fixed, the Li−N distances in complex YLi···NH_2X (Y = Cl, Br, or I) decrease with the order NH_2F > NH_2Cl > NH_2Br > NH_2I. The weaker the electronegativity of the halogen in NH_2X, the stronger the interaction between the lithium and nitrogen atoms. There are also reasonable correlations between the complexation enthalpies and the electronegativity of X (Figure 2, $R^2 = 0.867$ for LiCl, and correlation coefficients are even greater for LiBr and LiI). It is noteworthy that the complexation enthalpies for FLi···NH_2X (X = F, Cl, Br, or I) decrease from 67.1 (X = F) to 63.4 kJ/mol (X = I), which can be explained by a small change in the Li−N distance and a significant increase in the F−H distances from 2.440 Å in complex FLi···NH_2F to 2.786 Å in FLi···NH_2I. The interactions between the fluoride anion and two hydrogen atoms seem to override the contribution from the Li−N interaction. The shorter the bond distance of F−H, the higher the complexation enthalpy.

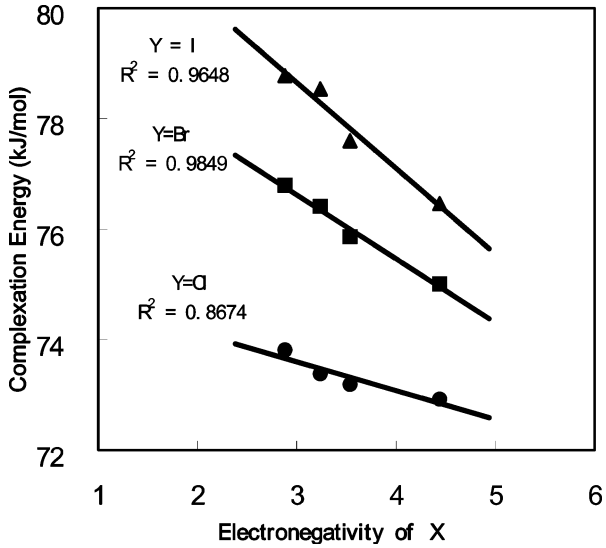

Figure 2. Plot of G2M(+) complexation enthalpies for dipole−dipole complexes YLi···NH_2X (X = F−I) vs Mulliken electronegativities of X (in Pauling units). ΔH^{comp}_{YX} and ΔH^{comp}_{XY} values are listed in Table 2.

C. Transition-State Structures and Barrier Heights. The inversion transition-state structures $[LiY/NH_2X]^{‡}$ (Y ≠ X, Y, X = F, Cl, Br, or I) are found to have C_s symmetry. In these TS structures, lithium coordinates with nitrogen, acts as a bridge connecting both halogen atoms, and causes a slight deformation from the TS geometries found in anionic S_N2 reactions at nitrogen.[2c] The bridging actions of the Li cation cause the two halogen anions to bend toward it with a decrease of the X−N−X angle by ca. 35°, which is much different from the inversion TS structures $[LiX/CH_3X]^{‡}$ (X = F, Cl, Br, or I),[11a] where there is a remarkable deformation from the linear geometry found in $[X\cdots CH_3\cdots X]^{-‡}$ and the Li cation causes a large decrease of the X−C−X angle by ca. 80°. These may be the main reasons why the activation barriers for the ion pair S_N2 reactions at nitrogen are much lower than the corresponding values at carbon (see Table 3). The Li−N interactions also contribute to the stability of the transition-state structures because the Li^+ attacks the lone pair of nitrogen atoms and, thus, increases the electrophilicity of the nitrogen center in the transition state.

The main geometric feature in inversion transition-state structures $[LiY/NH_2X]^{‡}$ is the simultaneous elongation of the Li−Y and N−X bonds relative to the dipole−dipole complex. We can easily characterize the geometric looseness of the Li−Y and N−X bonds in the TS structures by the parameters %Li−$Y^{‡}$ and %N−$X^{‡}$, in a way similar to that proposed by Shaik et al.[22a]

$$\%Li-Y^{‡} = 100*[r^{‡}(Li-Y) - r^{comp}(Li-Y)]/[r^{comp}(Li-Y)] \quad (3)$$

$$\%N-X^{‡} = 100[r^{‡}(N-X) - r^{comp}(N-X)]/[r^{comp}(N-X)] \quad (4)$$

where $r^{‡}$(Li−Y) and $r^{‡}$(N−X) are the bond lengths in the transition structure **2** and r^{comp}(Li−Y) and r^{comp}(N−X) are those in dipole−dipole complex **1** for the Li−Y and N−X bonds, respectively.

The search for relationships between transition-state structures and reaction barriers is an important aspect of physical organic chemistry. Such relationships are of particular interest because of their extensive use by scientists. The geometric looseness in S_N2 TS structures gives an indication of the extent of bond

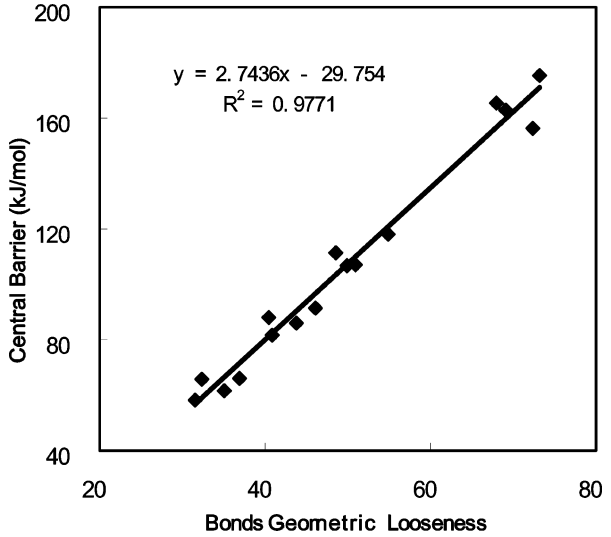

Figure 3. Plot of G2M(+) central barriers ($\Delta H^{\ddagger}_{YX}$ and $\Delta H^{\ddagger}_{XY}$) for eqs 1 and 2 vs the sum of geometric looseness of Li−Y and N−X bonds of the transition structures **2**. $\Delta H^{\ddagger}_{YX}$ and $\Delta H^{\ddagger}_{XY}$ values are listed in Table 2. The B3LYP/6-311+G(d,p) values of %Li−Y‡ and %N−X‡ are presented in Figure 1.

TABLE 4: Calculated G2M(+) Heterolytic Cleavage Energies (kJ/mol) for Reactions $NH_2X \rightarrow NH_2^+ + X^-$ [$\Delta H_{het}(NH_2X)$] and $LiX \rightarrow Li^+ + X^-$ [$\Delta H_{het}(LiY)$]

X	G2M(+)[a] $\Delta H_{het}(NH_2X)$	G2M(+)[b] $\Delta H_{het}(NH_2X)$	G2M(+) $\Delta H_{het}(LiX)$
F	1035.5	1034.1	738.3
Cl	985.1	982.6	621.7
Br	973.3	970.9	588.7
I	976.7	977.7	557.2

[a] Energies of the reactions $NH_2X \rightarrow NH_2^+(^3B_1) + X^-$. The lowest singlet ($^1A_1$) state of NH_2^+ lies 110.9 kJ/mol above the $^3B_1$ ground state at the G2M(+) level. [b] From ref 2a.

weakening. Computations on nonidentity S_N2 reactions at carbon[21] and at nitrogen[2e] have revealed that the geometric looseness of the TS structures correlates with the magnitude of the central barrier. Present calculated results show that a larger barrier is associated with a transition state having higher percentages of Li−Y and N−X bond lengthening. As illustrated in Figure 3, the sum of %Li−Y‡ and %N−X‡ correlates well with the magnitude of the central barrier ($R^2 = 0.977$). This correlation indicates that the stretching of the cleaving Li−Y and N−X bonds is the major factor determining the central barrier heights ($\Delta H^{\ddagger}_{YX}$ and $\Delta H^{\ddagger}_{XY}$). The other two factors may be the heterolytic cleavage energies (see Table 4) for the reactions $NH_2X \rightarrow NH_2^+ + X^-$ [$\Delta H_{het}(NH_2X)$] and $LiY \rightarrow Li^+ + Y^-$ [$\Delta H_{het}(LiY)$]. This is reasonable because the central barrier heights in the LiY + NH_2X (Y, X = F−I) reactions should also be governed by the energies of the ionic cleavage reactions. There is still a good linear relationship ($R^2 = 0.966$) between $\Delta H^{\ddagger}_{YX}$ and (%Li−Y‡)$\Delta H_{het}(LiY)$ + (%N−X‡)ΔH_{het}-(NH_2X). It is obvious that the looseness of the transition state will be dominant due to the smaller relative differences between the heterolytic cleavage energies.

Comparison of the forward overall barriers for the LiY + NH_2X (Y, X = F, Cl, Br, or I) reactions with the corresponding predicted values (see Table 3) in the Y^- + NH_2X reactions indicates that all of the overall barriers, $\Delta H^{\ddagger}_{IX}$, for the forward reactions of LiI + NH_2X (X = F, Cl, Br, or I) are lower than those in the anionic S_N2 reactions. Meanwhile, we notice that the overall barriers for other reactions, LiY + NH_2X (Y, X = F, Cl, or Br) and LiY + NH_2I (Y = F, Cl, or Br), are higher than those in the anionic S_N2 reactions. These results show that the dissociation energies, D_{Li-Y}, or the heterolytic cleavage energies, ΔH_{het}(LiY), for Li−Y (Y = F−I) bonds play an important role in determining the barrier heights. The weakest Li−I bond and the smallest %Li−I‡ value may be responsible for the lower overall barrier for the inversion [LiI/NH_2X]‡ TS. Plots of the inversion overall barrier for TS [LiY/NH_2X]‡ versus ΔH_{het}(LiY) or D_{Li-Y} (where Y = F, Cl, Br, or I) generate good linear correlations ($R^2 > 0.98$). All of the above results mean that the introduction of a lithium cation will raise the overall barriers for the LiY + NH_2X (Y, X = F, Cl, or Br) reactions and lower the overall barrier for the LiI + NH_2X (X = F−I) reactions, which suggest that the forward ion pair reactions involving the iodine may be a more facile process than anionic ones I^- + NH_2X (X = F−I).

It is also shown in Table 3 that all of the overall barriers for LiY/CH_3X are significantly higher than those in the LiY + NH_2X (Y, X = F, Cl, Br, or I) reactions. The barrier differences are from 40.2 (Y = F and X = I) to 160.2 kJ/mol (Y = I and X = F). These results imply that the ion pair S_N2 reactions at nitrogen will be significantly faster than the corresponding reactions at carbon in the gas phase, which is similar to the previous experimental results[2d] and theoretical predictions[2a] in anionic S_N2 reactions, where nucleophilic substitution at nitrogen is more facile than at carbon.

Calculated central barriers relative to complexes $\Delta H^{\ddagger}_{YX}$ and $\Delta H^{\ddagger}_{XY}$ for the ion pair reactions LiY + NH_2X (Y, X = F, Cl, Br, or I) at the level of G2M(+) span a large range from 58.2 kJ/mol for the LiI + NH_2Br reaction to 175.3 kJ/mol for the LiF + NH_2I reaction. According to the Marcus theory,[12a−c] in an exothermic reaction, a thermodynamic driving force will lower the transition-state energy, whereas the endothermic driving force will induce a higher activation energy. Therefore, the forward central barrier heights ($\Delta H_{YX}^{\ddagger}$) should be lower than the intrinsic central barrier ($\Delta H_0^{\ddagger}{}_{YX}$), and the reverse central barrier heights ($\Delta H_{XY}^{\ddagger}$) should be higher than the intrinsic central barrier ($\Delta H_0^{\ddagger}{}_{YX}$). $\Delta H_0^{\ddagger}{}_{YX}$ is estimated using the additivity postulate (eq 5). The G2M(+) central barriers in Table 3 show that all of the reactions, regardless of forward and reverse direction, are in agreement with the Marcus theory.

$$\Delta H_0^{\ddagger}{}_{YX} = {}^1/_2(\Delta H^{\ddagger}_{YY} + \Delta H^{\ddagger}_{XX}) \quad (5)$$

D. Application of the Marcus Theory. The Marcus theory has been successfully applied to methyl transfer reactions.[21] We also completed the extended application of the Marcus theory in the anionic S_N2 reactions at nitrogen.[2c] It will be interesting to test the reliability of the Marcus theory for the ion pair S_N2 reactions at nitrogen. The Marcus equation

$$\Delta H^{\ddagger}_{YX} = {}^1/_2(\Delta H^{\ddagger}_{YY} + \Delta H^{\ddagger}_{XX} + \Delta H) + [(\Delta H)^2/8(\Delta H^{\ddagger}_{YY} + \Delta H^{\ddagger}_{XX})] \quad (6)$$

relates the intrinsic barrier heights of a nonidentity displacement, $\Delta H^{\ddagger}_{YX}$, to the intrinsic barrier heights of the degenerate reactions, $\Delta H^{\ddagger}_{YY}$ and $\Delta H^{\ddagger}_{XX}$, and to the central enthalpy difference, ΔH. The data in Table 3 show that all of the Marcus-theory predicted values are slightly lower than the calculated G2M(+) central barrier heights by a few kilojoules per mole. The largest differences, mean signed error (MSE), and mean unsigned error (MUE) are −4.9, −2.4, and −2.4 kJ/mol, respectively, justifying the use of the Marcus equation for this purpose. A plot of the Marcus central barriers (by eq 6) versus

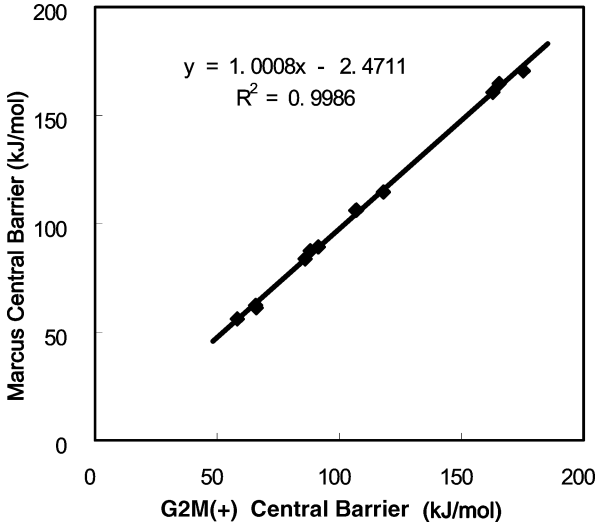

Figure 4. Plot of central barriers from eq 6 vs the same quantity obtained directly from the G2M(+) theory for the LiY + NH_2X (Y, X = F−I) reactions. All of the central barriers are presented in Table 3.

the G2M(+) data for the reactions LiY + NH_2X (Y, X = F−I) gives a very good linear correlation (Figure 4, $R^2 = 0.999$).

To apply the Marcus equation to the overall barriers, rather than the central barrier, Wolfe et al.[23] proposed the following modifications:

$$\Delta H^{b}_{YX} = \Delta H_0{}^{b}_{YX} + 0.5\Delta H^{ovr} + (\Delta H^{ovr})^2/16\Delta H_0{}^{\ddagger}_{YX} \quad (7)$$

$$\Delta H_0{}^{b}_{YX} = 0.5(\Delta H^{b}_{YY} + \Delta H^{b}_{XX}) \quad (8)$$

Equation 7 permits the predictions of the experimentally more accessible quantity from data of the corresponding identity reactions. The data in Table 3 illustrate the applicability of the Wolfe et al. equation to all of the nonidentity ion pair S_N2 reactions at nitrogen. Inspection of the results in Table 3 shows that the Wolfe et al. modification to the Marcus equation leads to very good predicted overall barriers, ΔH^{b}_{YX} and ΔH^{b}_{YX}, with the largest difference, MSE, and MUE values being −6.2, −2.9, and −2.9 kJ/mol, respectively. There is still a good correlation between the overall barriers obtained by the Wolfe et al. equation versus the G2M(+) calculated values ($R^2 = 0.998$) for eq 2. This is better than the corresponding correlation that existed in the nonidentity S_N2 reactions at carbon ($R^2 = 0.990$),[21] which may be attributed to the smaller exothermicity in eq 2. The successful application of the Marcus theory and its modification to the LiY + NH_2X (Y, X = F−I) reactions indicates that we can predict the reaction barrier heights for other nonidentity ion pair S_N2 reactions at nitrogen using the reaction barriers of identity reactions if the nonidentity reactions are not strongly exothermic.

E. Nucleophilicity of Lithium Halides in Gas-Phase Ion Pair S_N2 Reactions at Nitrogen. The order of nucleophilicity of nucleophiles is essential for describing S_N2 reactions and will strongly correlate with the rate ordering of the S_N2 reactions. Many properties have an influence on the nucleophilicity of an anion, such as the medium in S_N2 reactions, the strength of its bond with the central atom, and the electronegativity of the attacking atom. In the aliphatic anionic S_N2 reactions, the nucleophilicity of a nucleophile in the solvent may be different from that in the gas phase because of the solvation energy. The observed[24] and predicted [25a,b] reactivity sequences of nucleophiles in the gas-phase S_N2 reactions at carbon follow the order $F^- > Cl^- > Br^- > I^-$, which will be reverse in dipolar solvents, such as water and alcohol. In our previous study,[2e] we predicted the nucleophiles in the gas-phase anionic S_N2 reactions at nitrogen follow the same order as carbon. Here, we will discuss the nucleophilicity of different lithium halides in the gas-phase ion pair S_N2 reactions at nitrogen using our G2M(+) energetics in Table 3 and selected NBO analyses in Table 5.

1. Thermodynamic Study. As shown in previous work,[24] the exothermicity of the reactions of the nucleophile with a single substrate reflects the thermodynamic affinity of the nucleophile. Following this idea, the exothermal trend, in this work, is given by the sequences of the overall enthalpy change ΔH^{ovr} for the reaction as a function of nucleophile LiY. It can be seen from Table 3 that regardless of whichever LiY (F−I), reacts with any substrate, NH_2F, NH_2Cl, NH_2Br, or NH_2I, the exothermicity values falls in the same order LiI > LiBr > LiCl > LiF.

For example, ΔH^{ovr} values for the LiY + NH_2F (Y = F, Cl, Br, or I) reactions decrease in the order −122.4 (LiI) < −87.4 (LiBr) < −66.3 (LiCl) < 0 kJ/mol (LiF). This exothermicity can be clearly related to the nucleophilicity of LiY, decreasing in the trend LiI > LiBr > LiCl > LiF.

2. Kinetic Study. The high-level computational study of Glukhovtsev et al.[2a] for identity S_N2 reactions at nitrogen (eq 1) suggests that the more negative overall barrier heights, the more facile the S_N2 reactions. The overall barriers for reactions LiY + NH_2F (Y = F, Cl, Br, or I), as indicated in Table 3, show that the sequence given by ΔH^{b}_{YX} and ΔH^{b}_{XY} follows the order −10.4 (LiI) < 11.0 (LiBr) < 34.1 (LiCl) < 89.2 kJ/

TABLE 5: Selected Donor−Acceptor Interaction Energies, $E(2)$ (kcal/mol), for [LiY/NH_2Cl]‡ (Y = F−I) Transition-State Structures; MP2 Energies of NBO, E_{NBO} (au), for Donor and Acceptor; Energy Gap, ΔE_{NBO} (au), between Highest Orbital of Donor and Antibonding Orbital of N−Cl; Bond Order for N−Cl Bond, BO (N−Cl); and NPA Charge Distribution for Cl, q(Cl)

Y	NBO(donor)	E_{NBO}(donor)	NBO(acceptor)	E_{NBO}(acceptor)	$E(2)$	ΔE_{NBO}	BO(N−Cl)	q(Cl)
F	LP F	−0.55260	BD* N−Cl	−0.01819	170.9	0.53441	0.2255	−0.653
	LP F	−0.77334	BD* N−Cl	−0.01819	3.4			
	LP F	−1.25073	BD* N−Cl	−0.01819	10.9			
	LP N	−0.80829	LP* Li	0.20144	5.3			
Cl	LP Cl	−0.39364	BD* N−Cl	−0.05469	164.7	0.33895	0.2548	−0.565
	LP Cl	−0.53622	BD* N−Cl	−0.05469	2.2			
	LP Cl	−0.98392	BD* N−Cl	−0.05469	6.3			
	LP N	−0.81931	LP* Li	0.17681	5.6			
Br	LP Br	−0.35322	BD* N−Cl	−0.04386	129.4	0.30936	0.2901	−0.493
	LP Br	−0.46694	BD* N−Cl	−0.04386	1.1			
	LP Br	−0.79673	BD* N−Cl	−0.04386	3.8			
	LP N	−0.81930	LP* Li	0.18679	5.2			
I	LP I	−0.32401	BD* N−Cl	−0.02920	95.3	0.29481	0.3326	−0.406
	LP I	−0.40779	BD* N−Cl	−0.02920	0.4			
	LP I	−0.71248	BD* N−Cl	−0.02920	2.7			
	LP N	−0.81507	LP* Li	0.18052	5.0			

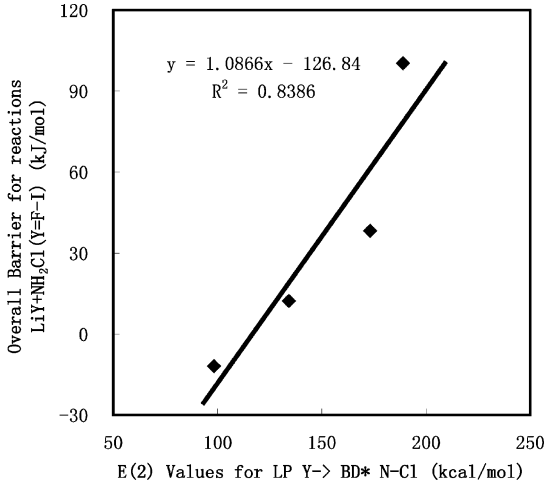

Figure 5. Plot of G2M(+) overall barriers for the LiY + NH_2Cl (Y = F−I) reactions vs the sum of the donor−acceptor interaction energies, *E*(2), for the interactions between the lone pair of Y and the antibonding orbital of the N−Cl bond.

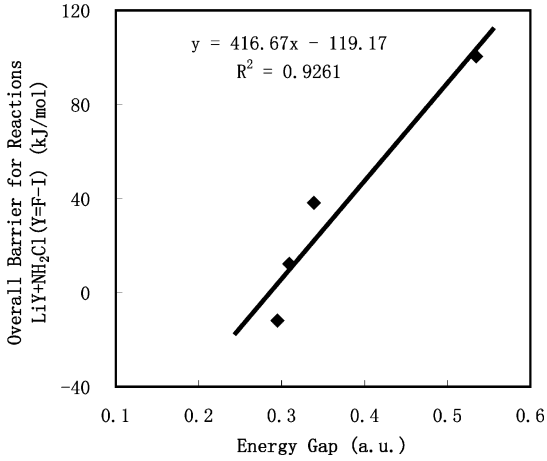

Figure 6. Plot of G2M(+) overall barriers for the LiY + NH_2Cl (Y = F−I) reactions vs the energy gaps between the highest NBO for the lone pair of Y and the antibonding orbital of the N−Cl bond.

mol (LiF), which is different from the order found in anionic S_N2 reaction at nitrogen,[2c] where the predicted nucleophilicity of halides in the gas phase follows in the order $F^- > Cl^- > Br^- > I^-$ based on analyses of the transition structures.

With the other three substrates, NH_2Cl, NH_2Br, and NH_2I, the same orders are also obtained. These results are in good agreement with the exothermicity of the reactions (eqs 1 and 2), showing the correlation between the overall activation barriers and the overall reaction enthalpies for the LiY + NH_2X (X = F, Cl, Br, or I) ($R^2 > 0.994$). That means that when the overall barriers decrease, the exothermicity of the reactions increases.

3. NBO Analysis. As shown in Table 5, among the TS structures $[LiY/NH_2Cl]^‡$ (Y = F−I), the main donor−acceptor interaction energies estimated by second-order perturbation theory, *E*(2), are from the interactions between a donor (a lone pair of attacking halogens, denoted as LP Y, Y = F, Cl, Br, or I) and an acceptor (antibonding orbital of N−Cl, denoted as BD* N−Cl), in which the interaction between the highest lone pair orbital of Y and BD* N−Cl will be dominant and determine the reaction barrier, following the order 170.9 (Y = F) > 164.7 (Y = Cl) > 129.4 (Y = Br) > 95.3 kcal/mol (Y = I).

Analyses of NPA and the bond order of the N−Cl bond (see Table 5) for the TS $[LiY/NH_2Cl]^‡$ (Y = F−I) indicate that the $[LiI/NH_2Cl]^‡$ TS more resembles the reagents (an early transition state) and the $[LiF/NH_2Cl]^‡$ TS more resembles the products (a late transition state). The later the transition state, the more electrons on the leaving halogen atom X; the higher the reaction barrier, the larger the *E*(2) value. The sums of *E*(2) between all three lone pairs on Y and the antibonding orbital of N−Cl, decreasing in the order 189.0 (Y = F) > 173.3 (Y = Cl) > 134.3 (Y = Br) > 98.4 kcal/mol (Y = I), are found to reasonably correlate with the overall activation barriers (Figure 5, $R^2 = 0.839$).

From the view of orbital interaction, the smaller energy gap, ΔE_{NBO}, between the highest orbital of the donor and antibonding orbital of N−Cl, will be favorable for the formation of a transition-state structure, leading to the lower activation barrier. A reasonable correlation between ΔE_{NBO} and the overall barriers for reactions LiY + NH_2Cl, ΔH^b_{YCl}, is observed (Figure 6, $R^2 = 0.926$).

In summary, the investigations of the kinetics and thermodynamics and NBO analyses lead to the same results. We attribute the different performance of LiY and Y^- in the order of nucleophilicity to the fact that the transition states $[LiY/NH_2X]^‡$ involve the breaking of the Li−Y bond, and the heterolytic cleavage energies of LiY decrease significantly from 738.3 kJ/mol in LiF to 557.2 kJ/mol in LiI. Clearly, the Li−Y electrostatic interaction will dominate the barrier heights. LiF has the highest heterolytic cleavage energy, and the formation of TS $[LiF/NH_2X]^‡$ is more difficult than other TS structures $[LiY/NH_2X]^‡$ (Y = Cl, Br, or I), which implies that LiF would prefer to be on the product side and LiI would prefer to be on the reactant side for all of the forward reactions, LiY + NH_2X → NH_2Y + LiX (Y is heavier than X). Therefore, the order of the nucleophilicity in gas-phase ion pair S_N2 reactions is expected to be the reverse for anionic reactions. The situation is analogous to the consideration of the nucleophilicity of a solvated anion. The Li^+ is such a strong cation that the nucleophilicity of the ion pairs is reversed from that of the free anions, similar to the reverse nucleophilicity order of halogen anions in the strong dipolar solvent from that in the gas phase as mentioned previously.

4. Conclusions

Application of the G2M(+) theory to gas-phase exchange reactions of lithium halide with amino halides, LiY + NH_2X → NH_2Y + LiX (Y, X = F−I), leads to the following conclusions:

(1) The energy profile is described by a double-well curve. The following channel for the model reactions is established. The enthalpies of reactions are exothermic only when the nucleophile is the heavier halide.

$$LiY + NH_2X \rightarrow YLi\cdots NH_2X \rightarrow [LiY/NH_2X]^‡ \rightarrow YH_2N\cdots LiX \rightarrow NH_2Y + LiX$$

(2) The complexation energies for complexes depend on the identity of LiY and are found to have inverse correlations with the electronegativities of the nucleophile.

(3) The forward central barrier heights, $\Delta H_{YX}^‡$, are lower than the intrinsic central barrier $\Delta H_0^‡{}_{YX}$, and the lowering is attributed to the effect of forward reaction exothermal behavior, which ranges from −21.1 kJ/mol for LiBr + NH_2Cl to −122.4 kJ/mol for LiI + NH_2F.

(4) The introduction of a lithium cation will raise the overall barriers for the LiY + NH_2X (Y, X = F, Cl, or Br) reactions

and lower the overall barrier for the LiI + NH_2Y reaction. All of the overall barriers are negative for the forward reactions involving the iodine (ΔH^b_{IX}) and positive for other reactions, which suggests that the reactions LiI + $NH_2X \rightarrow NH_2I$ + LiX (X = F−I) are more facile than others.

(5) Comparison of our computational barrier data for the LiY + NH_2X reactions with predicted results for LiY + CH_3X reactions shows that nucleophilic substitution at nitrogen is much faster than at carbon.

(6) The set of nonidentity reactions LiY + NH_2X (Y, X = F, Cl, Br, or I) obeys the Marcus equation and its modification. The central barriers estimated by the Marcus equation are close to the directly calculated central barrier, and a plot of the two data sets gives a good correlation. The overall barriers estimated by a modified Marcus equation are also found to reproduce the calculated results of G2M(+).

(7) Reaction barriers exhibit good linear relationships with the sum of the geometric looseness of Li−Y and N−X bonds in the transition structures. There is a correlation between forward overall barriers and overall enthalpy changes.

(8) Combining the kinetic, thermodynamic investigations and NBO analysis, we predict that the nucleophilicity for lithium halides in the gas-phase ion pair S_N2 reactions at nitrogen follows the order LiI > LiBr > LiCl > LiF, which is the reverse of the corresponding anionic S_N2 reactions.

Acknowledgment. Y.R. is thankful for the support from the Scientific Research Foundation for the Returned Chinese Scholars of State Education Ministry and Sichuan University. S.-Y.C. thanks NSC of Taiwan for their financial support. We express our gratitude to the referees for their valuable comments.

Supporting Information Available: All of the Cartesian coordinates of the optimized structures involved in the LiY + NH_2X (Y, X = F−I) reactions. This material is available free of charge via the Internet at http://pubs.acs.org.

References and Notes

(1) Williams, A. *Concerted Organic and Bio-Organic Mechanisms*; CRC Press LLC: Boca Raton, FL, 2000; Chapter 6, p 159.

(2) (a) Glukhovtsev, M. N.; Pross, A.; Radom, L. *J. Am. Chem. Soc.* **1995**, *117*, 9012. (b) Ren, Y.; Basch, H.; Hoz, S. *J. Org. Chem.* **2002**, *67*, 5891. (c) Yang, J.; Ren, Y.; Zhu, H.-J.; Chu, S.-Y. *Int. J. Mass Spectrom.* **2003**, *229*, 199. (d) Gareyev, R.; Kato, S.; Bierbaum, V. M. *J. Am. Soc. Mass Spectrom.* **2001**, *12*, 139. (e) Ren, Y.; Zhu, H.-J. *J. Am. Soc. Mass Spectrom.* **2004**, *15*, 673.

(3) (a) Mullhearn, D. C.; Bachrach, S. M. *J. Am. Chem. Soc.* **1996**, *118*, 9415. (b) Bachrach, S. M.; Gailbreath, B. D. *J. Org. Chem.* **2001**, *66*, 2005. (c) Bachrach, S. M.; Chamberlin, A. C. *J. Org. Chem.* **2003**, *68*, 4743.

(4) Ren, Y.; Wolk, J. L.; Hoz, S. *Int. J. Mass Spectrom.* **2002**, *220*, 1.

(5) Sølling, T. I.; Radom, L. *Int. J. Mass Spectrom.* **2001**, *210*−*211*, 1.

(6) Glover, S. A.; Mo, G. *J. Chem. Soc., Perkin Trans. 2* **2002**, 1728.

(7) (a) Winstein, S.; Savedoff, L. G.; Smith, S.; Stevens, I.-D. R.; Gall, J. S. *Tetrahedron Lett.* **1960**, 24. (b) Lai, Z.-G.; Westaway, K. C. *Can. J. Chem.* **1989**, *67*, 21.

(8) Harder, S.; Streitwieser, A.; Petty, J. T.; Schleyer, P. v. R. *J. Am. Chem. Soc.* **1995**, *117*, 3253.

(9) Streitwieser, A.; Choy, G.-S. C.; Abu-Hasanayn, F. *J. Am. Chem. Soc.* **1997**, *119*, 5013.

(10) Leung, S.-S. W.; Streitwieser, A. *J. Comput. Chem.* **1998**, *19*, 1325.

(11) (a) Ren, Y.; Chu, S.-Y. *J. Comput. Chem.* **2004**, *25*, 461. (b) Ren, Y.; Chu, S.-Y. *Chem. Phys. Lett.* **2003**, *376*, 524.

(12) (a) Marcus, R. A. *Annu. Rev. Phys. Chem.* **1964**, *15*, 155. (b) Marcus, R. A. *J. Phys. Chem.* **1968**, *72*, 891. (c) Albery, W. J. *Annu. Rev. Phys. Chem.* **1980**, *31*, 227.

(13) Mebel, A. M.; Morokuma, K.; Lin, M. C. *J. Chem. Phys.* **1995**, *103*, 7414.

(14) (a) Zhu, R. S.; Xu, Z. F.; Lin, M. C. *J. Chem. Phys.* **2002**, *116*, 7452. (b) Bui, B. H.; Zhu, R. S.; Lin, M. C. *J. Chem. Phys.* **2002**, *117*, 11188. (c) Tokmakov, I. V.; Park, J.; Gheyas, S.; Lin, M. C. *J. Phys. Chem. A* **1999**, *103*, 3636.

(15) Parthiban, S.; de Oliveira, G.; Martin, J.-M. L. *J. Phys. Chem. A* **2001**, *105*, 895.

(16) (a) Becke, A. D. *J. Chem. Phys.* **1993**, *98*, 5648. (b) Becke, A. D. *J. Chem. Phys.* **1992**, *96*, 2155. (c) Becke, A. D. *J. Chem. Phys.* **1992**, *97*, 9173.

(17) Lee, C.; Yang, W.; Parr, R. G. *Phys. Rev. B* **1988**, *37*, 785.

(18) Frisch, M. J.; Trucks, G. W.; Schlegel, H. B.; Scuseria, G. E.; Robb, M. A.; Cheeseman, J. R.; Zakrzewski, V. G.; Montgomery, J. A.; Stratmann, R. E., Jr.; Burant, J. C.; Dapprich, S.; Millam, J. M.; Daniels, A. D.; Kudin, K. N.; Strain, M. C.; Farkas, O.; Tomasi, J.; Barone, V.; Cossi, M.; Cammi, R.; Mennucci, B.; Pomelli, C.; Adamo, C.; Clifford, S.; Ochterski, J.; Petersson, G. A.; Ayala, P. Y.; Cui, Q.; Morokuma, K.; Malick, D. K.; Rabuck, A. D.; Raghavachari, K.; Foresman, J. B.; Cioslowski, J.; Ortiz, J. V.; Baboul, A. G.; Stefanov, B. B.; Liu, G.; Liashenko, A.; Piskorz, P.; Komaromi, I.; Gomperts, R.; Martin, R. L.; Fox, D. J.; Keith, T.; Al-Laham, M. A.; Peng, C. Y.; Nanayakkara, A.; Gonzalez, C.; Challacombe, M.; Gill, P.-M. W.; Johnson, B.; Chen, W.; Wong, M. W.; Andres, J. L.; Gonzalez, C.; Head-Gordon, M.; Replogle, E. S.; Pople, J. A. *Gaussian 98*, revision A.9; Gaussian, Inc.: Pittsburgh, PA, 1998.

(19) Wadt, W. R.; Hay, P. J. *J. Chem. Phys.* **1985**, *82*, 284.

(20) (a) Reed, A. E.; Weinstock, R. B.; Weinhold, F. *J. Chem. Phys.* **1985**, *83*, 735. (b) Foster, J. P.; Weinhold, F. *J. Am. Chem. Soc.* **1980**, *102*, 7211. (c) Reed, A. E.; Weinhold, F. *J. Chem. Phys.* **1983**, *78*, 4066. (d) Reed, A. E.; Curtiss, L. A.; Weinhold, F. *Chem. Rev.* **1988**, *88*, 899.

(21) Glukhovtsev, M. N.; Pross, A.; Radom, L. *J. Am. Chem. Soc.* **1996**, *118*, 6273.

(22) Shaik, S. S.; Schlegel, H. B.; Wolfe, S. *J. Chem. Soc., Chem. Commun.* **1988**, 1322.

(23) Wolfe, S.; Mitchell, D. J.; Schlegel, H. B. *J. Am. Chem. Soc.* **1981**, *103*, 7694.

(24) Olmstead, W. N.; Brauman, J. I. *J. Am. Chem. Soc.* **1977**, *99*, 4219.

(25) (a) Shaik, S. S.; Hiberty, P. C. *Adv. Quantum Chem.* **1995**, *26*, 99. (b) Safi, B.; Choho, K.; Geerlings, P. *J. Phys. Chem. A* **2001**, *105*, 591.